

**DEVELOPMENT OF POLYMER/Al-Ag-ZnO  
NANOCOMPOSITES FOR UV-SHIELDING  
APPLICATIONS**

**HAMEED NASER KHALAF KHALAF**

**UNIVERSITI SAINS MALAYSIA**

**2025**

**DEVELOPMENT OF POLYMER/Al-Ag-ZnO  
NANOCOMPOSITES FOR UV-SHIELDING  
APPLICATIONS**

by

**HAMEED NASER KHALAF KHALAF**

**Thesis submitted in fulfilment of the requirements  
for the degree of  
Doctor of Philosophy**

**April 2025**

## ACKNOWLEDGEMENT

In the name of Allah, Most Gracious, Most Merciful

First, I must say "Alhamdulillah" and express my gratitude to the Almighty God for providing me with the courage, strength, patience, and resolve necessary to finish my doctoral studies.

I am incredibly thankful to my main supervisor, Dr. Sabah M. Mohammad, for his wonderful academic guidance, ongoing support, and intellectual encouragement for my doctoral work and associated research.

Additionally, I am deeply grateful to my co-supervisor, Dr. Haider Mohammed Shanshool, for generously sharing his professional expertise with me during my research. He dedicated a significant amount of time and effort to guide me through the process of conducting research and writing academic papers.

I want to thank my co-supervisor, Prof. Dr. Zainuriah Hassan, for all the support, encouragement, time, comments, recommendations, and help she has given me.

I also want to thank my wonderful wife, my two boys, and my three daughters for their patience, support, understanding, and the great environment they created while I worked on this project. Thank you to everyone who worked at NOR Lab, especially Mr. Abdul Jamil Yusuf, Mr. Yushamdan Yusof, and others, for all the technical help and advice you gave me on my journey here. Finally, I thank everyone I've met at INOR and Physics School.

Hameed Naser Khalaf Khalaf

Penang, Malaysia. 2025

## TABLE OF CONTENTS

<b>ACKNOWLEDGEMENT</b> .....	<b>ii</b>
<b>TABLE OF CONTENTS</b> .....	<b>iii</b>
<b>LIST OF TABLES</b> .....	<b>x</b>
<b>LIST OF FIGURES</b> .....	<b>xi</b>
<b>LIST OF SYMBOLS</b> .....	<b>xvi</b>
<b>LIST OF ABBREVIATIONS</b> .....	<b>xvii</b>
<b>ABSTRAK</b> .....	<b>xviii</b>
<b>ABSTRACT</b> .....	<b>xx</b>
<b>CHAPTER 1 INTRODUCTION</b> .....	<b>1</b>
1.1 Introduction.....	1
1.2 Problem Statement .....	2
1.3 Research Objectives .....	4
1.4 Thesis Originality.....	5
1.5 Thesis Overview .....	5
<b>CHAPTER 2 LITERATURE REVIEW</b> .....	<b>7</b>
2.1 Introduction.....	7
2.2 Background of Polymers.....	7
2.3 Nanoparticles .....	8
2.4 Background of Insulation Polymers.....	10
2.5 Insulator-to-Conductor Polymer Conversion.....	11
2.6 Linear Optical Properties of Nanocomposites .....	14
2.6.1 Linear Optical Properties of Polystyrene.....	14
2.6.1(a) Linear Optical Properties of Polystyrene with Single Nanoparticle .....	15

2.6.1(b)	Linear Optical Properties of Polystyrene with Bimetallic Nanoparticle.....	17
2.6.2	Linear Optical Properties of Poly (methyl methacrylate).....	20
2.6.2(a)	Linear Optical Properties of Poly (methyl methacrylate) with a Single Nanoparticle .....	20
2.6.2(b)	Linear Optical Properties of Poly (methyl methacrylate) with a Bimetallic Nanoparticle.....	22
2.6.3	Linear Optical Properties of Poly (vinyl alcohol) .....	24
2.6.3(a)	Linear Optical Properties of Poly (vinyl alcohol) with a Single Nanoparticle .....	25
2.6.3(b)	Linear Optical Properties of Poly (vinyl alcohol) with a Bimetallic Nanoparticle.....	28
2.7	Casting Method.....	31
2.8	Shielding for UV Region .....	32
<b>CHAPTER 3 METHODOLOGY .....</b>		<b>35</b>
3.1	Introduction.....	35
3.2	Preparation Method.....	37
3.3	Materials .....	37
3.3.1	Polymers .....	37
3.3.2	Metal and Metal Oxide NPs .....	37
3.3.3	Solvents .....	38
3.4	Preparation of Polymer/Al, Polymer/Ag, and Polymer/ZnO NCs Foils.....	38
3.5	Preparation of Polymer/ (Al+Ag) NCs, Polymer/ (Al+ZnO) NCs, and Polymer/ (Ag+ZnO) NCs Foils.....	42
3.6	Characterization Methods .....	44
3.6.1	Field Emission Scanning Electron Microscope (FESEM) .....	44
3.6.2	AFM.....	45
3.6.3	FTIR.....	47

3.6.4	UV-Vis Spectroscopy .....	48
3.6.5	Set Up of Optical UV Shielding.....	49
<b>CHAPTER 4 RESULTS AND DISCUSSION.....</b>		<b>51</b>
4.1	Introduction.....	51
4.2	Structural and Morphological of Synthesized PS, PMMA, and PVA Nanocomposites .....	51
4.2.1	Transmission Electron Microscopy (TEM) Images of the Nanoparticle Material of Al, Ag, and ZnO NPs .....	51
4.2.2	FESEM and EDX Analysis .....	52
4.2.2(a)	FESEM and EDX for PS/Al, PS/Ag, and PS/ZnO NCs.....	53
4.2.2(b)	FESEM and EDX for PMMA/Al, PMMA/Ag, and PMMA/ZnO NCs .....	54
4.2.2(c)	FESEM and EDX for PVA/Al, PVA/Ag, and PVA/ZnO NCs .....	55
4.2.3	Top View FESEM Images and EDS Analysis .....	56
4.2.3(a)	Top View FESEM and EDS for PS/(Al+Ag), PS/(Al+ZnO), and PS/(Ag+ZnO) NCs.....	56
4.2.3(b)	Top View FESEM and EDS for PMMA/(Al+Ag), PMMA/(Al+ZnO), and PMMA/(Ag+ZnO) NCs .....	57
4.2.3(c)	Top View FESEM and EDS for PVA/(Al+Ag), PVA/(Al+ZnO), and PVA/(Ag+ZnO) NCs.....	58
4.2.4	AFM Images and Topographical Analysis .....	60
4.2.4(a)	AFM 3D Images of the PS/(Ag+ZnO), PS/(Al+Ag), and PS/(Al+ZnO) NCs .....	60
4.2.4(b)	AFM 3D Images of the PMMA/(Ag+ZnO), PMMA/(Al+Ag), and PMMA/(Al+ZnO) NCs .....	60
4.2.4(c)	AFM 3D Images of the PVA/(Ag+ZnO), PVA/(Al+Ag), and PVA/(Al+ZnO) NCs.....	61
4.3	FTIR Spectroscopy Analysis .....	62

4.3.1	FTIR Analysis for PS/Al, PS/Ag, PS/ZnO, and PS/(Ag+ZnO), PS/(Al+Ag), PS/(Al+ZnO) NCs .....	62
4.3.2	FTIR Analysis for PMMA/Al, PMMA/Ag, PMMA/ZnO, and PMMA/(Ag+ZnO), PMMA/(Al+Ag), PMMA / (Al+ZnO) NCs .....	63
4.3.3	FTIR Analysis for PVA/Al, PVA/Ag, PVA/ZnO, and PVA/(Ag+ZnO), PVA/(Al+Ag), PVA/(Al+ZnO) NCs.....	65
4.4	Linear Optical Properties .....	67
4.4.1	Transmittance (T) .....	67
4.4.1(a)	The Transmittance spectra of PS/Al, PS/Ag, PS/ZnO, and PS/(Al+Ag), PS/(Al+ZnO), PS/(Ag+ZnO) NCs .....	67
4.4.1(b)	The Transmittance spectra of PMMA/Al, PMMA/Ag, PMMA/ZnO, and PMMA/(Al+Ag), PMMA/(Al+ZnO), PMMA/(Ag+ZnO) NCs.....	68
4.4.1(c)	The Transmittance spectra of PVA/Al, PVA/Ag, PVA/ZnO, and PVA/(Al+Ag), PVA/(Al+ZnO), PVA/(Ag+ZnO).....	70
4.4.2	Absorption (A).....	71
4.4.2(a)	The Absorption spectra of PS/Al, PS/Ag, PS/ZnO, and PS/(Ag+ZnO), PS/(Al+Ag), PS/(Al+ZnO) NCs.....	71
4.4.2(b)	The Absorption spectra of PMMA/Al, PMMA/Ag, PMMA/ZnO, and PMMA/(Ag+ZnO), PMMA/(Al+Ag), PMMA/(Al+ZnO) NCs .....	72
4.4.2(c)	The Absorption spectra of PVA/Al, PVA/Ag, PVA/ZnO, and PVA/(Ag+ZnO), PVA/(Al+Ag), PVA/(Al+ZnO) NCs.....	74
4.4.3	Reflectance (R) .....	75
4.4.3(a)	The Reflectance Spectra of PS/Al, PS/Ag, PS/ZnO, and PS/(Ag+ZnO), PS/(Al+Ag), PS/(Al+ZnO) NCs .....	75
4.4.3(b)	The Reflectance Spectra of PMMA/Al, PMMA/Ag, PMMA/ZnO, and	

	PMMA/(Ag+ZnO), PMMA/(Al+Ag), PMMA/(Al+ZnO) NCs .....	77
4.4.3(c)	The Reflectance Spectra of PVA/Al, PVA/Ag, PVA/ZnO, and PVA/(Ag+ZnO), PVA/(Al+Ag), PVA/(Al+ZnO) NCs.....	79
4.4.4	Linear Absorption Coefficient ( $\alpha$ ) .....	80
4.4.4(a)	The Linear Absorption Coefficient of PS/Al, PS/Ag, PS/ZnO, and PS/(Ag+ZnO), PS/(Al+Ag), PS/(Al+ZnO) NCs .....	81
4.4.4(b)	The Linear Absorption Coefficient of PMMA/Al, PMMA/Ag, PMMA/ZnO, PMMA/(Ag+ZnO), PMMA/(Al+Ag), PMMA/(Al+ZnO) NCs .....	82
4.4.4(c)	The Linear Absorption Coefficient of PVA/Al, PVA/Ag, PVA/ZnO, PVA/(Ag+ZnO), PVA/(Al+Ag), PVA/(Al+ZnO) NCs.....	83
4.4.5	Energy Band Gap ( $E_g$ ) .....	85
4.4.5(a)	The Energy Band Gap of PS/Al, PS/Ag, PS/ZnO, and PS/(Ag+ZnO), PS/(Al+Ag), and PS/(Al+ZnO) NCs .....	85
4.4.5(b)	The Energy Band Gap of PMMA/Al, PMMA/Ag, PMMA/ZnO, and PMMA/(Ag+ZnO), PMMA/(Al+Ag), PMMA/(Al+ZnO) NCs .....	88
4.4.5(c)	The Energy Band Gap of PVA/Al, PVA/Ag, PVA/ZnO, and PVA/(Ag+ZnO), PVA/(Al+Ag), PVA/(Al+ZnO) NCs.....	90
4.4.6	Extinction Coefficient ( $K$ ) .....	93
4.4.6(a)	The Extinction Coefficient of PS/Al, PS/Ag, PS/ZnO, and PS/(Ag+ZnO), PS/(Al+ZnO), PS/(Al+Ag) NCs.....	93
4.4.6(b)	The Extinction Coefficient of PMMA/Al, PMMA/Ag, PMMA/ZnO, and PMMA/(Ag+ZnO), PMMA/(Al+Ag), PMMA/(Al+ZnO) NCs .....	94
4.4.6(c)	The Extinction Coefficient of PVA/Al, PVA/Ag, PVA/ZnO, and PVA/(Ag+ZnO), PVA/(Al+Ag), PVA/(Al+ZnO) NCs.....	96

4.4.7	Refractive Index (n).....	97
4.4.7(a)	The Refractive Index of PS/Al, PS/Ag, PS/ZnO, and PS/(Ag+ZnO), PS/(Al+ZnO), PS/(Al+Ag) NCs.....	98
4.4.7(b)	The Refractive Index of PMMA/Al, PMMA/Ag, PMMA/ZnO, and PMMA/(Ag+ZnO), PMMA/(Al+Ag), PMMA/(Al+ZnO) NCs.....	99
4.4.7(c)	The Refractive Index of PVA/Al, PVA/Ag, PVA/ZnO, and PVA/(Ag+ZnO), PVA/(Al+Ag), PVA/(Al+ZnO) NCs.....	101
4.4.8	Optical Dielectric Constant .....	102
4.4.8(a)	The Optical Dielectric Constant of PS/Al, PS/Ag, PS/ZnO, and PS/ (Ag+ZnO), PS/ (Al+ZnO), PS/ (Al+Ag) NCs .....	103
4.4.8(b)	The Optical Dielectric Constant of PMMA/Al, PMMA/Ag, PMMA/ZnO, and PMMA/(Ag+ZnO), PMMA/(Al+Ag), PMMA/(Al+ZnO) NCs .....	105
4.4.8(c)	The Optical Dielectric Constant of PVA/Al, PVA/Ag, PVA/ZnO, and PVA/(Ag+ZnO), PVA/(Al+Ag), PVA/(Al+ZnO) NCs.....	107
4.4.9	Optical Conductivity ( $\sigma_{opt}$ ) Study.....	108
4.4.9(a)	The Optical Conductivity of PS/Al, PS/Ag, PS/ZnO, and PS/(Ag+ZnO), PS/(Al+ZnO), PS/(Al+Ag) NCs.....	109
4.4.9(b)	The Optical Conductivity of PMMA/Al, PMMA/Ag, PMMA/ZnO, and PMMA/(Ag+ZnO), PMMA/(Al+Ag), PMMA/(Al+ZnO) NCs .....	110
4.4.9(c)	The Optical Conductivity of PVA/Al, PVA/Ag, PVA/ZnO, and PVA/(Ag+ZnO), PVA/(Al+Ag), PVA/(Al+ZnO) NCs.....	112
4.5	Optical UV- shielding .....	113
4.5.1	Effects of Different Concentrations of Al, Ag, and ZnO in NCs .....	113
4.5.2	Effects of Different Bimetallic NPs in NCs .....	115

4.6	Summary .....	118
<b>CHAPTER 5 CONCLUSION AND FUTURE STUDIES.....</b>		<b>120</b>
5.1	Conclusion .....	120
5.2	Future Studies .....	123
<b>REFERENCES.....</b>		<b>124</b>
<b>LIST OF PUBLICATIONS</b>		

## LIST OF TABLES

	<b>Page</b>
Table 2.1	Summary of previous review articles on polystyrene with a single material nanoparticle ..... 17
Table 2.2	Summary of previous review articles on polystyrene with a bimetallic material nanoparticle..... 19
Table 2.3	Summary of previous review articles on Poly (methyl methacrylate) with a single material nanoparticle. .... 22
Table 2.4	Summary of previous review articles on Poly (methyl methacrylate) with a bimetallic material nanoparticle..... 24
Table 2.5	Summary of previous review articles on poly (vinyl alcohol) with a single material nanoparticle. .... 28
Table 2.6	Summary of previous review articles on poly (vinyl alcohol) with a bimetallic material nanoparticle..... 30
Table 3.1	Prepared single nanocomposites. .... 41
Table 3.2	Prepared bimetallic nanocomposites..... 43

## LIST OF FIGURES

		Page
Figure 2.1	Different ways to synthesize nanoparticles [31].	10
Figure 2.2	Electronically conductive polymer band structure.	13
Figure 2.3	Illustrates the process of polaron and bipolaron formation in polyacetylene.	13
Figure 2.4	Illustrates the casting method of preparation of the foils.	31
Figure 2.5	Visualises the different strata of the skin under the influence of ultraviolet (UV) radiation [122].	34
Figure 3.1	Flowchart for characterization of the prepared samples of this work.	36
Figure 3.2	Preparation method of PS/Al NCs, PMMA/Al NCs, PVA/Al NCs, PS/Ag NCs, PMMA/Ag NCs, PVA/Ag NCs, PS/ZnO NCs, PMMA/ZnO NCs, and PVA/ZnO NCs.	41
Figure 3.3	Preparation method of polymer/ (Al+Ag) NCs, polymer/ (Al+ZnO) NCs, and polymer/ (Ag+ZnO) NCs.	43
Figure 3.4	A diagram of the FESEM [124].	45
Figure 3.5	Schematic of an atomic force microscope. A cantilever's deflection can be observed when a sample presses down on its tip, which is mounted on top of it [126].	47
Figure 3.6	FTIR system optical schematic [131].	48
Figure 3.7	UV-Vis spectrophotometer schematic [133].	49
Figure 3.8 (a)	Experimental setup for UV shielding.	50
Figure 3.8 (b)	Top view real image of the experimental setup for the application of UV shielding.	50
Figure 4.1	TEM images of the nanoparticle material showing (a) Al NPs, (b) Ag NPs, (c) ZnO NPs spheroidal nature.	52
Figure 4.2	EDX spectra of (a) PS/Al, (b) PS/Ag, (c) PS/ZnO NCs.	54
Figure 4.3	EDX spectra of (a) PMMA/ Al NCs, (b) PMMA/Ag NCs, and (c) PMMA/ZnO NCs.	55

Figure 4.4	EDX spectra of (a) PVA/Al NCs, (b) PVA/Ag NCs, (c) PVA/ZnO NCs.....	56
Figure 4.5	Top view FESEM images of NCs (a) PS/(Al+Ag), (b) PS/(Al+ZnO), and (c) PS/(Ag+ZnO) with EDS chemical mapping.....	57
Figure 4.6	Top view FESEM images with EDS elemental mapping of NCs (a) PMMA/(Al+Ag), (b) PMMA/(Al+ZnO), and (c) PMMA/(Ag+ZnO). ....	58
Figure 4.7	Top view FESEM images with EDS elemental mapping of NCs (a) PVA/(Al+Ag), (b) PVA/(Al+ZnO), and (c) PVA/(Ag+ZnO). ....	59
Figure 4.8	Shows AFM 3D images of the samples (a) PS/(Ag+ZnO) NCs, (b) PS/(Al+Ag) NCs, and (c) PS/(Al+ZnO) NCs. The scanned region measures 5 $\mu\text{m}$ $\times$ 5 $\mu\text{m}$ . ....	60
Figure 4.9	Shows AFM 3D images of the samples (a) PMMA/(Ag+ZnO) NCs, (b) PMMA/(Al+Ag) NCs, and (c) PMMA/(Al+ZnO) NCs. The scanned region measures 5 $\mu\text{m}$ $\times$ 5 $\mu\text{m}$ . ....	61
Figure 4.10	Shows AFM 3D images of the samples (a) PVA/(Ag+ZnO) NCs, (b) PVA/(Al+Ag) NCs, and (c) PVA/(Al+ZnO) NCs. The scanned region measures 5 $\mu\text{m}$ $\times$ 5 $\mu\text{m}$ .....	62
Figure 4.11	Displays the FTIR spectra of three different nanocomposites: (a) PS/Al, (b) PS/Ag, (c) PS/ZnO, (d) PS/(Ag+ZnO), PS/(Al+Ag), PS/(Al+ZnO). ....	63
Figure 4.12	Displays the FTIR spectra of three different nanocomposites: (a) PMMA/Al, (b) PMMA/Ag, (c) PMMA/ZnO, (d) PMMA/(Ag+ZnO), PMMA/(Al+Ag), PMMA/(Al+ZnO). ....	65
Figure 4.13	Displays the FTIR spectra of three different nanocomposites: (a) PVA/Al, (b) PVA/Ag, (c) PVA/ZnO, (d) PVA/(Ag+ZnO), PVA/(Al+Ag), PVA/(Al+ZnO). ....	66
Figure 4.14	Optical transmittance against wavelength for PS Pure, (a) PS/Al, (b) PS/Ag, (c) PS/ZnO, and (d) PS/(Al+Ag), PS/(Al+ZnO), PS/(Ag+ZnO) NCs. ....	68
Figure 4.15	Optical transmittance against wavelength for PMMA Pure (a) PMMA/Al, (b) PMMA/Ag, (c) PMMA /ZnO, and (d) PMMA/(Al+Ag), PMMA/(Al+ZnO), PMMA/(Ag+ZnO) NCs. ....	70
Figure 4.16	Optical transmittance against wavelength for PVA Pure, (a) PVA/Al, (b) PVA/Ag, (c) PVA/ZnO, and (d) PVA/(Al+Ag), PVA/(Al+ZnO), PVA/(Ag+ZnO) NCs.....	71

Figure 4.17	Absorption as a function of wavelength for NCs (a) PS/Al, (b) PS/Ag, (c) PS/ZnO, (d) PS/(Ag+ZnO), PS/(Al+Ag), PS/(Al+ZnO).....	72
Figure 4.18	Absorption as a function of wavelength for NCs (a) PMMA/Al, (b) PMMA/Ag, (c) PMMA/ZnO, (d) PMMA/(Ag+ZnO), PMMA/(Al+Ag), PMMA/(Al+ZnO).....	73
Figure 4.19	Absorption as a function of wavelength for NCs (a) PVA/Al, (b) PVA/Ag, (c) PVA/ZnO, (d) PVA/(Ag+ZnO), PVA/(Al+Ag), PVA/(Al+ZnO). ....	75
Figure 4.20	Displays the reflectance spectra of nanocomposites, namely (a) PS/Al, (b) PS/Ag, (c) PS/ZnO, (d) PS/(Ag+ZnO), PS/(Al+Ag), and PS/(Al+ZnO).....	77
Figure 4.21	Displays the reflectance spectra of nanocomposites, namely (a) PMMA/Al, (b) PMMA/Ag (c) PMMA/ZnO, PMMA/(Ag+ZnO), PMMA/(Al+Ag), and PMMA/(Al+ZnO).....	78
Figure 4.22	Exhibits the reflectance spectra of nanocomposites, namely (a) PVA/Al (b) PVA/Ag, (c) PVA/ZnO, PVA/(Ag+ZnO), PVA/(Al+Ag), and PVA/(Al+ZnO).....	80
Figure 4.23	Plot of linear absorption coefficient against wavelength for nanocomposites (a) PS/Al, (b) PS/Ag, (c) PS/ZnO, (d) PS/(Ag+ZnO), PS/(Al+Ag), PS/(Al+ZnO).....	82
Figure 4.24	Plot of linear absorption coefficient against wavelength for nanocomposites (a) PMMA/Al, (b) PMMA/Ag, (c) PMMA/ZnO, (d) PMMA/(Ag+ZnO), PMMA/(Al+Ag), PMMA/(Al+ZnO).....	83
Figure 4.25	Plot of linear absorption coefficient against wavelength for nanocomposites (a) PVA/Al, (b) PVA/Ag, (c) PVA/ZnO, (d) PVA/(Ag+ZnO), PVA/(Al+Ag), PVA/(Al+ZnO).....	84
Figure 4.26	Plot of $(\alpha hv)^2$ against $hv$ for nanocomposites (a) PS/Al, (b) PS/Al, and (c) PS/Al, (d) PS/(Ag+ZnO), PS/(Al+Ag), PS/(Al+ZnO).....	87
Figure 4.27	Schematic representations of the band structures of PS, with integrated Al, Ag, ZnO, (Ag+ZnO), (Al+Ag), (Al+ZnO) NCs. ....	87
Figure 4.28	Plot of $(\alpha hv)^2$ against $hv$ for nanocomposites (a) PMMA/Al (b) PMMA/Ag, (c) PMMA/ZnO, (d) PMMA/(Ag+ZnO), PMMA/(Al+Ag), PMMA/(Al+ZnO).....	89

Figure 4.29	Schematic representations of the band structures of PMMA, with integrated Al, Ag, ZnO, (Ag+ZnO), (Al+Ag), (Al+ZnO) NCs. ....	90
Figure 4.30	Plot of $(\alpha hv)^2$ against $hv$ for nanocomposites (a) PVA/Al (b) PVA/Ag, (c) PVA/ZnO, (d) PVA/(Ag+ZnO), PVA/(Al+Ag), PVA/(Al+ZnO). ....	92
Figure 4.31	Schematic representations of the band structures of PVA, with integrated Al, Ag, ZnO, (Ag+ZnO), (Al+Ag), (Al+ZnO) NCs. ....	92
Figure 4.32	The variation in the extinction coefficient (k) for the (a) PS/Al NCs, (b) PS/Ag NCs, (c) PS/ZnO NCs, (d) PS/(Ag+ZnO) NCs, PS/(Al+ZnO) NCs, PS/(Al+Ag) NCs with wavelength.....	94
Figure 4.33	The variation in the extinction coefficient (k) for the (a) PMMA/Al NCs, (b) PMMA/Ag NCs, (c) PMMA/ZnO NCs, (d) PMMA/(Ag+ZnO) NCs, PMMA/(Al+ZnO) NCs, PMMA/(Al+Ag) NCs with wavelength. ....	95
Figure 4.34	The variation in the extinction coefficient (k) for the (a) PVA/Al NCs, (b) PVA/Ag NCs, (c) PVA/ZnO V, (d) PVA/(Ag+ZnO)NCs, PVA/(Al+ZnO) NCs, PVA/(Al+Ag) NCs with wavelength. ....	97
Figure 4.35	Displays the refractive index of nanocomposites, specifically (a) PS/Al, (b) PS/Ag, (c) PS/ZnO, (d) PS/(Ag+ZnO), PS/(Al+Ag), PS/(Al+ZnO). ....	99
Figure 4.36	Displays the refractive index of nanocomposites, specifically (a) PMMA/Al, (b) PMMA/Ag, (c) PMMA/ZnO, (d) PMMA/(Ag+ZnO), PMMA/(Al+Ag), PMMA/(Al+ZnO). ....	100
Figure 4.37	Displays the refractive index of nanocomposites, specifically (a) PVA/Al, (b) PVA/Ag, (c) PVA/ZnO, (d) PVA/(Ag+ZnO), PVA/(Al+Ag), PVA/(Al+ZnO). ....	102
Figure 4.38	Displays both the real and imaginary parts of the dielectric constant as a function of wavelength for nanocomposites: (a) PS/Al, (b) PS/Ag, (c) PS/ZnO, (d) PS/(Ag+ZnO), PS/(Al+Ag), PS/(Al+ZnO).....	104
Figure 4.39	Displays both the real and imaginary parts of the dielectric constant as a function of wavelength for nanocomposites: (a) PMMA/Al, (b) PMMA/Ag, (c) PMMA/ZnO, (d) PMMA/(Ag+ZnO), PMMA/(Al+Ag), PMMA/(Al+ZnO). ....	106

Figure 4.40	Displays both the real and imaginary parts of the dielectric constant as a function of wavelength for nanocomposites: (a) PVA/Al, (b) PVA/Ag, (c) PVA/ZnO, (d) PVA/(Ag+ZnO), PVA/(Al+Ag), PVA/(Al+ZnO) .	108
Figure 4.41	The optical conductivity versus wavelength for pure and doped (a) PS/Al, (b) PS/Ag, (c) PS/ZnO, (d) PS/(Ag+ZnO), PS/(Al+Ag), PS/(Al+ZnO) NCs.	110
Figure 4.42	The optical conductivity versus wavelength for pure and doped (a) PMMA/Al, (b) PMMA/Ag, (c) PMMA/ZnO, (d) PMMA/(Ag+ZnO), PMMA/(Al+Ag), PMMA/(Al+ZnO) NCs. ....	111
Figure 4.43	The optical conductivity versus wavelength for pure and doped (a) PVA/Al, (b) PVA/Ag, (c) PVA/ZnO, (d) PVA/(Ag+ZnO), PVA/(Al+Ag), PVA/(Al+ZnO) NCs. ....	113
Figure 4.44	Output power of PS, blend Al, Ag, ZnO NPs doped as foils.....	114
Figure 4.45	Output power of PMMA, blend Al, Ag, ZnO NPs doped as foils. ....	115
Figure 4.46	Output power of PVA, blend Al, Ag, ZnO NPs doped as foils. ....	115
Figure 4.47	Output power of PS, blend (Al+Ag), (Al+ZnO), (Ag+ZnO) NPs doped as foils. ....	117
Figure 4.48	Output power of PMMA, blend (Al+Ag), (Al+ZnO), (Ag+ZnO) NPs doped as foils.....	117
Figure 4.49	Output power of PVA, blend (Al+Ag), (Al+ZnO), (Ag+ZnO) NPs doped as foils.....	117

## LIST OF SYMBOLS

A	Absorbance
T	Transmittance
R	Reflectance
n	Refractive Index
K	Extinction Coefficient
$\alpha$	Linear Absorption Coefficient
$E_g$	Band Gap Energy
$\epsilon$	Optical Dielectric Constant
$\sigma_{opt}$	Optical Conductivity
h	Planck's constant
$\lambda$	Wavelength
Wt%	Weight percentage
m	Mass
$\mu$	Density
v	Volume
CHCl <sub>3</sub>	Chloroform
C <sub>7</sub> H <sub>8</sub>	Toluene
H <sub>2</sub> O	Water
eV	Electron volt
°C	Celsius temperature
rpm	Angular velocity
RT	Room temperature
d	Thickness

## LIST OF ABBREVIATIONS

a. u.	Arbitrary unit
AFM	Atomic Force Microscopy
RMS	Root Mean Square
NCs	Nanocomposites
NPs	Nanoparticles
CV	Conduction band
EDS	Elemental mapping
EDX	Energy dispersive X-ray
FESEM	Field emission scanning electron microscopy
FTIR	Fourier transform infrared
HOMO	Highest occupied molecular orbital
LUMO	Lowest unoccupied molecular orbital
PMMA	Poly (methyl methacrylate)
PS	Polystyrene
PVA	Polyvinyl alcohol
UV	Ultraviolet
UV-Vis	Ultraviolet-visible
VB	Valence band
IR	Infrared radiation
Ag	Silver
Al	Aluminium
ZnO	Zinc oxide

# PEMBANGUNAN NANOKOMPOSIT POLIMER/Al-Ag-ZnO UNTUK APLIKASI PERISAI-UV

## ABSTRAK

Tesis ini membentangkan pembangunan nanokomposit (NCs) polimer/aluminium (Al)-perak (Ag)-zink oksida (ZnO) dengan konfigurasi logam-tunggal (Al, Ag, atau ZnO) atau dwilogam (Al+Ag, Al+ZnO, dan Ag+ZnO) untuk aplikasi perisai-ultraungu (UV). Teknik tuangan digunakan untuk fabrikasi nanozarah (NPs) (Al-Ag-ZnO), (Al+Ag), (Al+ZnO) dan (Ag+ZnO) berbentuk-kerajang yang fleksibel. NPs (Al-Ag-ZnO) ditambah sebagai pengisi pada 0, 1, 5, 10, dan 15 %berat, manakala (Al+Ag), (Al+ZnO), dan (Ag+ZnO) dengan 5 %berat kepada matriks polimer seperti polivinil alkohol (PVA), polimetil metakrilat (PMMA), dan polistirena (PS). Morfologi NPs Al, Ag dan ZnO, dengan julat saiz 20 hingga 160 nm, dianalisis menggunakan teknik mikroskopi pemancaran elektron (TEM). Pemeriksaan penyebaran tenaga sinar-X (EDX) menunjukkan kehadiran NPs Al, Ag, dan ZnO dengan kepekatan yang berbeza-beza dan mengesahkan penyebarannya di dalam matriks polimer. Spektra pemancaran UV-cahaya nampak menunjukkan pancaran rendah dalam julat UV, dengan arah aliran yang bertentangan diperhatikan relatif kepada kepekatan NPs. Spektra penyerapan UV-cahaya nampak menunjukkan penyerapan yang tinggi di kawasan UV, yang berkaitan secara songsang dengan kehadiran NCs (Al+Ag), (Al+ZnO), dan (Ag+ZnO). Pekali penyerapan linear ( $\alpha$ ) digunakan untuk menunjukkan kehadiran pinggir serapan. Semasa pengiraan jurang jalur tenaga, didapati semua NCs mempamerkan anjakan merah dalam jurang jalur tenaga mereka. Akibatnya, jurang jalur tenaga mengurang kepada 4.09 eV, 4.49 eV

dan 4.73 eV untuk NCs 15 %berat bagi PS/Al, PMMA/Al dan PVA/Al, masing-masing. Jurang jalur tenaga bagi NCs 15 %berat mengurang kepada 4.08 eV, 4.50 eV dan 4.80 eV untuk PS/Ag, PMMA/Ag dan PVA/Ag, masing-masing. Jurang jalur tenaga optik bagi NCs 15 %berat ialah 3.87 eV untuk PS/ZnO, 4.64 eV untuk PMMA/ZnO, dan 4.67 eV untuk PVA/ZnO, masing-masing. Selain itu, nilai jurang jalur tenaga untuk semua sampel mengurang apabila NPs (Al+Ag), (Al+ZnO), dan (Ag+ZnO) dicampur dengan polimer. Akibatnya, jurang tenaga berkurangan daripada 4.45 kepada 3.15 eV, terutamanya apabila polimer dicampur dengan NPs (Ag+ZnO). Pemantulan ( $R$ ), pekali kepupusan ( $K$ ), indeks biasan linear ( $n$ ), bahagian nyata ( $\epsilon^r$ ), khayalan ( $\epsilon^i$ ) bagi pemalar dielektrik, dan kekonduksian optik ( $\sigma_{opt}$ ) bagi NCs yang terhasil telah dinilai dan dianalisis. Meningkatkan kepekatan Al, Ag, dan ZnO membawa kepada peningkatan dalam semua parameter yang diukur. Semua nanokomposit yang disintesis mempunyai pemantulan UV yang tinggi tetapi pemantulan cahaya nampak yang rendah, terutamanya apabila dicampur dengan NPs Ag atau Al. Nilai indeks biasan yang diramalkan untuk nanokomposit yang dicadangkan adalah melebihi 1.5, menunjukkan kesan ketara daripada NPs ZnO, Al, dan Ag. Parameter optik adalah tertinggi untuk NCs polimer/(Ag+ZnO) dan terendah untuk NCs polimer/(Al+Ag). Spektra perisai bagi PS, PMMA, dan PVA yang didopkan dengan Al, Ag, dan ZnO menunjukkan pengurangan ketara dalam pemancaran pada cahaya laser dengan panjang gelombang 355 nm. Pemancaran nanozarah dwilogam menunjukkan pengurangan ketara berbanding dengan bahan nanokomposit lain yang disediakan dan ini mencadangkan NCs PS/(Ag+ZnO) adalah sangat efektif bagi aplikasi perisai UV.

# DEVELOPMENT OF POLYMER/Al-Ag-ZnO NANOCOMPOSITES FOR UV-SHIELDING APPLICATIONS

## ABSTRACT

This thesis presented the development of polymer/ aluminum (Al)-silver (Ag)-zinc oxide (ZnO) nanocomposites (NCs) with single-metal (Al, Ag, or ZnO) or bimetallic (Al+Ag), (Al+ZnO), and (Ag+ZnO) configurations for ultraviolet (UV)-shielding applications. The casting technique was employed for the fabrication of flexible foil-shaped (Al-Ag-ZnO), (Al+Ag), (Al+ZnO), and (Ag+ZnO) nanoparticles (NPs). The (Al-Ag-ZnO) NPs added as filler at 0, 1, 5, 10, and 15 wt%, while (Al+Ag), (Al+ZnO), and (Ag+ZnO) with 5 wt% to polymer matrices such as polyvinyl alcohol (PVA), polymethyl methacrylate (PMMA), and polystyrene (PS). The morphology of Al, Ag, and ZnO NPs, with a size range of 20 to 160 nm, was analyzed using the transmission electron microscopy (TEM) technique. Energy dispersive X-ray (EDX) examination showed the presence of Al, Ag, and ZnO NPs in the samples at different concentrations, confirming their dispersion inside the polymer matrix. UV-visible transmittance spectra showed low transmittance in the UV range, with a contrasting trend observed relative to NPs concentrations. UV-visible absorption spectra showed high absorption in the UV region, which was inversely related to the presence of (Al+Ag), (Al+ZnO), and (Ag+ZnO) NCs. A linear absorption coefficient ( $\alpha$ ) was used to demonstrate the presence of absorption edges. During the calculation of the energy band gap, it was found that all NCs exhibited a redshift in their energy band gaps. As a result, the energy band gap decreased to 4.09 eV, 4.49 eV, and 4.73 eV for the 15 wt% NCs of PS/Al, PMMA/Al, and PVA/Al, respectively. The energy band gaps of the 15 wt% NCs decreased to 4.08 eV, 4.50 eV, and 4.80 eV for PS/Ag, PMMA/Ag,

and PVA/Ag, respectively. The optical energy band gaps of the 15 wt% NCs were 3.87 eV for PS/ZnO, 4.64 eV for PMMA/ZnO, and 4.67 eV for PVA/ZnO, respectively. Additionally, the energy band gap values for all samples decreased when (Al+Ag), (Al+ZnO), and (Ag+ZnO) NPs were mixed with the polymers. As a result, the energy gap decreased from 4.45 to 3.15 eV, especially when the polymer was mixed with (Ag+ZnO) NPs. The reflectance ( $R$ ), extinction coefficient ( $K$ ), linear refractive index ( $n$ ), real ( $\epsilon^r$ ), imaginary ( $\epsilon^i$ ) parts of dielectric constants, and optical conductivity ( $\sigma_{opt}$ ) of the resulting NCs were evaluated and analyzed. Increasing the concentrations of Al, Ag, and ZnO NPs led to an increase in all the measured parameters. All synthesized nanocomposites had high UV reflectivity but low visible light reflectivity, especially when the polymer was mixed with Ag or Al NPs. The predicted refractive index values for the suggested nanocomposites were above 1.5, indicating a significant impact from the ZnO, Al, and Ag NPs. The optical parameters were highest for the polymer/(Ag+ZnO) NCs and lowest for the polymer/(Al+Ag) nanocomposites. The shielding spectra of PS, PMMA, and PVA mixed with Al, Ag, and ZnO NPs showed a significant reduction in transmittance at the laser light of 355 nm wavelength. The transmittance of bimetallic nanoparticles decreased significantly with PS/(Ag+ZnO) NCs compared to other prepared nanocomposite materials, suggesting that PS/(Ag+ZnO) NCs are highly effective for UV shielding applications.

# CHAPTER 1

## INTRODUCTION

### 1.1 Introduction

Recently, significant attention has been paid to polymer nanocomposites (NCs) in science and technology. These composite materials, known as nanocomposites, are made up of nanoparticles (NPs), which are nanometer-sized and distributed throughout a polymer matrix. The polymer and the nanoparticles' characteristics were altered when they were added to a matrix of polymers. The result was an enhanced nanocomposite and the possibility of developing novel technological applications [1]. Combining polymers with nanoparticles made materials with enhanced mechanical, electrical, optical, magnetic, thermal, and many other qualities possible. Therefore, their impact on composite characteristics is either improved or precisely realized at lower filler concentrations [2]. A single material with unique characteristics could be synthesized by effectively combining materials with disparate properties to synthesize nanocomposites. This material has applications in several scientific domains and could be utilized to synthesize high-performance new materials. However, polymers play important roles in many fields and are widely used in optoelectronics due to their low cost, lightweight, and flexibility.

Nanocomposites' optical characteristics have shown a lot of interest because they are different from individual polymers and have special properties that distinguish them from conventional materials [3]. Many factors, such as the size of the filler, size distribution, degree of dispersion, and filler contents, certainly influence the optical properties of nanocomposites [4].

The size of the nanoparticles, such as nanofillers, was a crucial factor influencing several aspects of the optical properties of nanocomposites. [1]. The most recent study claims that because these nanoparticles are much smaller than the wavelength of light, they reduce the amount of light that scatters. It was found in sizes between 50 and 100 nm. Therefore, nanoparticle-containing nanocomposites behave as optically homogenous materials that change optical characteristics, attracting the interest of researchers. Previous studies [5, 6] reported that an absorption peak was red-shifted depending on the size of the nanoparticles [7]. Typically, polymers have a refractive index of 1.3 to 1.5; however, adding nanoparticles could raise this value to 2.5 [8].

In another study, the preparation of polyaniline/Zn/Al NCs for the study of their optical properties revealed results that showed those nanocomposites could be used as protection for UV spectrum [9]. On the other hand, preparing a hybridization of silver (Ag) and zinc oxide (ZnO) could significantly improve ZnO's photocatalytic activity [10, 11]. The relationship between UV shielding and photocatalytic activity is primarily linked to the role of ZnO and Ag NPs in light absorption, charge carrier dynamics, and material stability. While my primary focus is on UV shielding, the photocatalytic properties of ZnO and Ag NPs influence the overall performance of the nanocomposite. So far, polymer/ZnO-Al NCs or polymer/ZnO-Ag NCs have been studied in different applications. This thesis combines polymer/ZnO-Ag with Al NPs to obtain new optical properties of nanocomposites for UV-shielding applications.

## **1.2 Problem Statement**

Technological and well-known scientists have studied nanocomposites prepared as thin film deposition on the substrate for the last few years.

This work used the casting method to prepare nanocomposites of polymer/ZnO, Al, and Ag NPs with single and bimetallic materials as foils.

Materials Today Journal [12] has called zinc oxide the material of the twenty-first century. ZnO NPs: Their excellent UV shielding is due to their high absorption and scattering efficiency in terms of optical properties. Their wide band gap also contributes to their transparency in the visible spectrum. Nonetheless, further data and understanding of ZnO and its nanocomposites' linear optical characteristics are required [12, 13].

It has been discovered that aluminium nanoparticles, or Al NPs, have unique optical properties for use in optoelectronic applications, including broad-band wire-grid polarizers [14], metal-enhanced fluorescence for label-free biomolecule detection [15], and surface-enhanced Raman scattering (SERS) [16]. Due to its high reflectivity, especially for visible and ultraviolet light, it is perfect for use as a reflecting surface [17].

Silver nanoparticles Ag NPs are among the most studied systems, and they are still attractive due to their potential applications [18]. Ag NPs are reported to emit photoluminescence in the UV visible spectrum at room temperature [19].

To obtain the best performance, it is necessary to solve the numerous issues associated with developing polymer nanocomposites with Al, Ag, or ZnO NPs foils to enhance optical qualities. Reduced efficiency and scattering losses can result from non-uniform dispersion. The stability and endurance of the composite under different environmental conditions depend on the strong interfacial connection between the material nanoparticles and the polymer matrix. Another challenging problem is the precise control of the optical properties of material nanoparticles.

These factors significantly affect the overall optical performance. These challenges must be resolved to create high-performance nanocomposites that can be used in UV shielding applications and sophisticated optical devices [20].

This work fills the need to study the linear optical properties of polymer/Al-Ag-ZnO NCs. The research proposal on optical linearity is essential for developing new materials for UV-shielding applications. To our knowledge, no literature describing the synthesis of polymer/Al-Ag-ZnO NCs as foils.

### 1.3 Research Objectives

This thesis carries three objectives, as follows:

1. To study the impact of varying concentrations of Al, Ag, and ZnO as single and bimetallic nanoparticles on the morphological and linear optical properties of polystyrene (**PS**), polymethyl methacrylate (**PMMA**), and polyvinyl alcohol (**PVA**) as foil nanocomposites prepared by casting method.
2. To compute and investigate the essential functional parameters of linear optical properties of the synthesized polymer nanocomposites such as transmittance (T), absorption (A), reflectance (R), linear absorption coefficient ( $\alpha$ ), energy band gap (Eg), extinction coefficient (K), refractive index (n), dielectric constant ( $\epsilon$ ), and optical conductivity ( $\sigma_{opt}$ ).
3. To evaluate and develop the optical properties of PS, PMMA, and PVA - single and bimetallic nanoparticles nanocomposites for UV-shielding applications.

#### 1.4 Thesis Originality

The following points summarized the originality of this research result:

1. To the best of my knowledge, no literature reported the synthesis of (Al+ZnO), (Al+Ag), or (Ag+ZnO) NPs as matrix fillers in PS, PMMA, or PVA nanocomposites and studying their linear optical properties.
2. The novel Nanoparticles are used with organic/inorganic nanocomposites such as polymer/Al, polymer/Ag, polymer/ZnO, and polymer/(Al+Ag), polymer/(Al+ZnO), and polymer/(Ag+ZnO) NCs in optoelectronics and UV-shielding applications.
3. An innovative idea to develop a novel nanocomposite by mixing nanoparticles of materials has developed.

#### 1.5 Thesis Overview

This thesis has been divided into five chapters, and the following explains how it is organized: **Chapter 1** introduces the optical properties of nanocomposite materials Al, Ag, and ZnO. The problem statement identifies the research objectives and thesis originality. **Chapter 2** gives the Literature Review, which explains deeply the properties and fabrication methods of Al, Ag, and ZnO NPs. It also provides further details on the background of insulation polymers, the linear optical properties of polymers with a single material, and the linear optical properties of polymers with a bimetallic structure. In addition, it discusses the casting method for preparing the foils and UV-shielding applications. **Chapter 3** details the methods used to conduct the experiments explained in this thesis. It also outlines the working principle of the equipment utilized to collect results and the type of characterizations.

The data from the collection and discussion of the measurement findings are presented in **Chapter 4**. This chapter presents and discusses the results. It analyses the structural and morphological characteristics of nanocomposites' linear optical properties and their application in optical UV shielding. **Chapter 5** concludes the thesis. It summarizes the key characteristics and limitations of the nanocomposites' linear optical properties and offers recommendations for further research.

## **CHAPTER 2**

### **LITERATURE REVIEW**

#### **2.1 Introduction**

This chapter presents the study's history. It summarises the linear optical properties of polymer/Al-Ag-ZnO NCs: first, as pure and mixing polymer; second, as polymer/bimetallic NCs. Nanocomposites are polymers or metals with nanoparticles (1–100 nm). These materials mix matrix and nanoparticle properties, usually delivering superior or unique characteristics. The properties of polymers are crucial for UV shielding applications. Due to their unique physicochemical properties, polymers like PS, PMMA, and PVA find widespread use in optical and protective applications. PS is an amorphous thermoplastic with excellent transparency and mechanical strength. However, it has limited UV stability and can degrade under prolonged UV exposure [21]. PMMA is a highly transparent polymer with strong UV resistance due to its inherent ability to absorb UV radiation below 300 nm. Its optical clarity makes it an ideal choice for UV-protective coatings and films[22].PVA has high film-forming ability, good mechanical strength, and hydrophilicity, making it suitable for coatings and composites. However, it requires reinforcement with UV-absorbing nanoparticles to enhance its UV-shielding efficiency [23].

#### **2.2 Background of Polymers**

The term "polymer" is derived from the Greek words "poly," which means "many," and "mer," which means "part." Consequently, a polymer is made up of segments—units that repeat regularly—that are connected by covalent bonds. The polymers are categorized into the following:

Two main categories of polymers come out of the polymerization process: homopolymers, which are compounds made up of several monomers, and copolymers, which are compounds made up of two or more different types of polymers linked together in a single chain. Polymers can be categorized according to their sources: natural, which comes from plants and animals, and synthetic, which is produced from simple industrial chemicals. Natural polymers include gum, rubber, cotton, wool, and leather. Based on the synthesis technique, polymers can be categorized as either addition polymers (where monomers are joined together to form a single product without losing any molecules) or condensation polymers (where monomers are introduced together with the removal of specific minor molecules, such as water).

Polymers are categorized into thermoplastic, elastomers, and thermosetting based on molecular forces, with thermoplastics softening or melting upon heating, elastomers being elastic, and thermosetting permanently changing upon heating. Based on their chemistry, polymers can be organic, inorganic, or element-organic and can include units with synthetic mineral elements and organic groups.

### **2.3 Nanoparticles**

In the early 20th century, Richard Zsigmondy made the first intentional observations and measurements of nanoparticles. He used an ultramicroscope to study gold sols (colloidal gold suspensions) and other materials. [24, 25]. Furthermore, modern nanoscience and nanotechnology have been greatly influenced by American physicist Richard Feynman's speech, "There is Plenty of Room at the Bottom," given on December 29, 1959, at the California Institute of Technology (Caltech) [26]. Many methods have been documented in the literature for synthesizing NPs ranging in size from 0.01 to 100 nm.

Nanoparticles are suited for various applications and exhibit novel and unparalleled properties compared to their bulk counterparts. [27]. However, depending on the synthesis technique, handling nanoscale components must be specialized and sophisticated. Properties of nanoparticles (Al, Ag, and ZnO) and their UV Shielding role. The incorporation of nanoparticles significantly enhances the UV-blocking efficiency of polymer matrices. ZnO is a wide-bandgap semiconductor ( $\sim 3.37$  eV) that effectively absorbs UV radiation, preventing its transmission through the material [28]. Due to its high absorption in the UV-A and UV-B regions, it is commonly used in UV shielding applications. In addition, Al NPs contribute to UV protection primarily by reflecting and scattering UV radiation. Studies have shown that Al-based nanocomposites can effectively reduce UV transmission when properly dispersed in polymers [29]. Also, Ag NPs have plasmonic resonance effects that make them absorb and scatter light strongly in the UV and visible ranges. Ag has been reported to enhance UV shielding when incorporated into polymer matrices [30]. Figure 2.1 displays two processes for synthesizing nanoparticles: bottom-up and top-down.

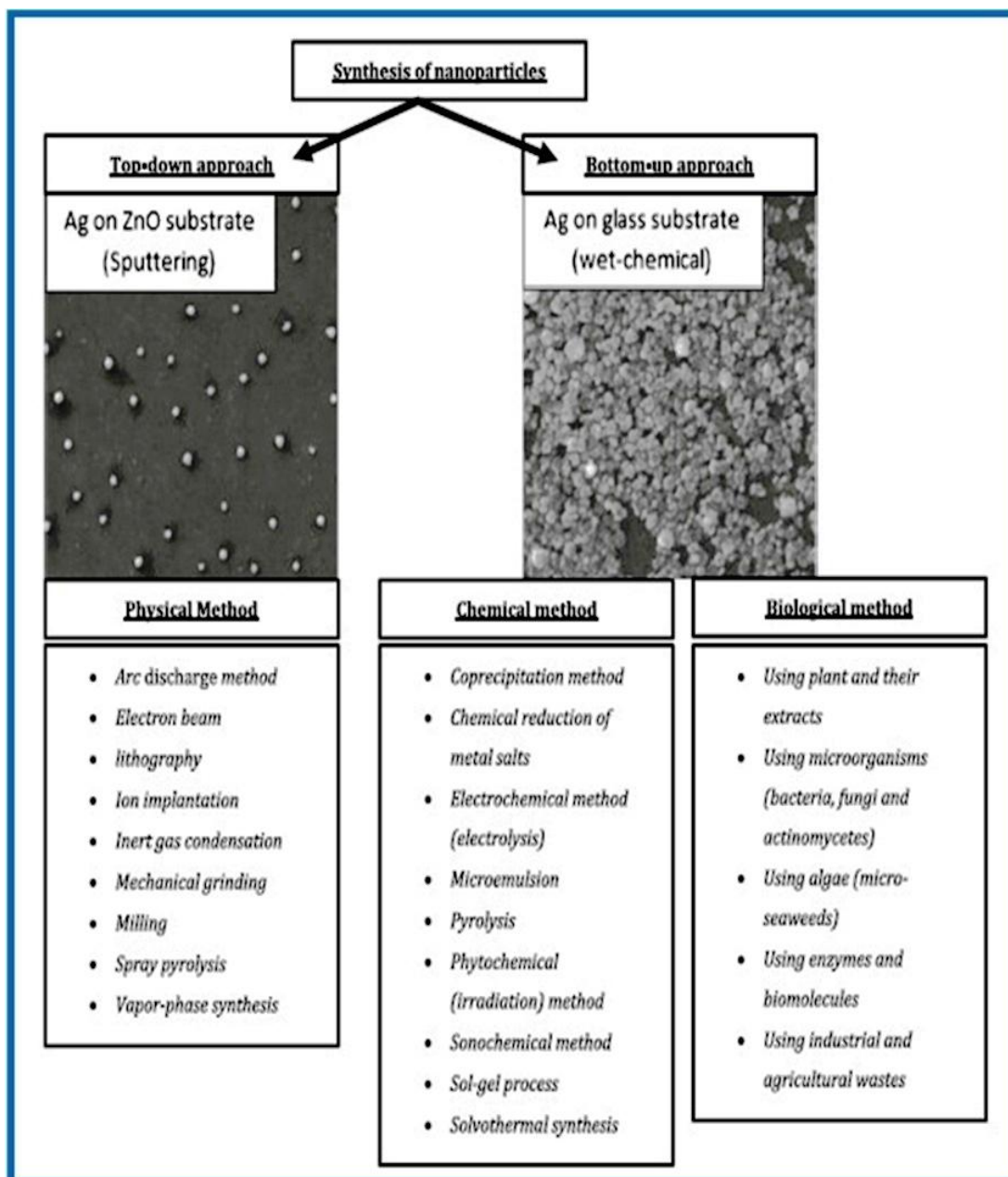


Figure 2.1 Different ways to synthesize nanoparticles [31].

## 2.4 Background of Insulation Polymers

Insulation polymers are compounds that reduce heat transfer, electricity, and sound. They are essential in various industries, including construction, electronics, and automotive. The following are insulating polymers, along with examples of their many applications.

Polyethylene (PE) is a low-density polyethylene (LDPE) that is used for electrical insulation, packaging, and films. High-density polyethylene (HDPE) is used for pipelines, cable insulation, and geomembranes [32]. Given its durability and fire resistance, Polyvinyl Chloride (PVC) is commonly used in electrical cable insulation, cables, and construction materials [33]. Polyurethane (PU) is used in rigid foam to provide thermal insulation in the building, refrigeration, and automotive industries. It offers excellent thermal insulation properties [34]. In fact, because of its chemical resistance and sound insulation properties, Polypropylene (PP) is used in various applications, including automotive parts, packaging, and electrical insulation [35]. On the other hand, Polyimide (PI) is known for its thermal resilience and is used in electronics to produce flexible printed circuit boards and insulating films. Fluor polymers are utilized in applications requiring high chemical resistance, low friction, and high-temperature stability, such as wire insulation and nonstick coatings [36]. In addition, Polyethylene Terephthalate (PET) is used in films for electrical insulation, packaging, and textile fibers due to its superior mechanical properties and stability [37].

## **2.5 Insulator-to-Conductor Polymer Conversion**

Conducting polymers may possess a transition from insulating to metal-like conductivity, with the exact transition occurring at the dopant chemical concentration. This property is controlled by adding impurities (dopants) to the polymer. The procedure that allows conducting polymers to become conductive, similar to a semiconductor, is the transfer of electrons from the valence band (VB) to the conduction band (CB) in response to temperature excitation [38]. An electrically conducting polymer band structure is illustrated in Figure 2.2.

The HOMO shows the highest occupied molecular orbital, and the LUMO the lowest unoccupied molecular orbital. Eg the energy gap, which is defined as the difference in energy between the HOMO and LUMO. The energy difference between the lowest unoccupied band (CB) and the highest occupied  $\pi$  electron band (VB) provides the essential optical characteristics of these materials [39, 40]. This idea could be applied to conductivity if the band gap is small. Nonetheless, when the band gap is enormous, and the energy needed for electrons to transmit across it at normal temperature is not satisfied, this hypothesis becomes useless. Consequently, research into charge carrier characteristics, in addition to band theory, is essential. The process of charge carrier formation in doped inorganic semiconductors can be used as a model for the n-type (electrons) or p-type (holes) charge carriers [38].

Figure 2.3 illustrates that the charge is accommodated in polaron states at low doping levels of polymers. A polaron is a quasiparticle formed when an electron or hole is associated with the lattice distortion resulting in a material. A localized deformation zone is formed when an electron distorts through a lattice due to interactions with its ions. While the polaron damages the lattice in its interaction, the electron energy is lowered compared to that of the unperturbed electron. A bipolaron is a pair of polarons (two electrons or two holes) that band together due to contact with the surrounding crystal lattice, significantly influencing the material's electrical and optical properties. However, it undergoes the bipolaron transition at high doping levels, a phenomenon where a defect is doubly charged. When an electric field is applied to a conjugated system, polarons and bipolarons may shift along the polymeric chain by rearranging the double and single bonds.

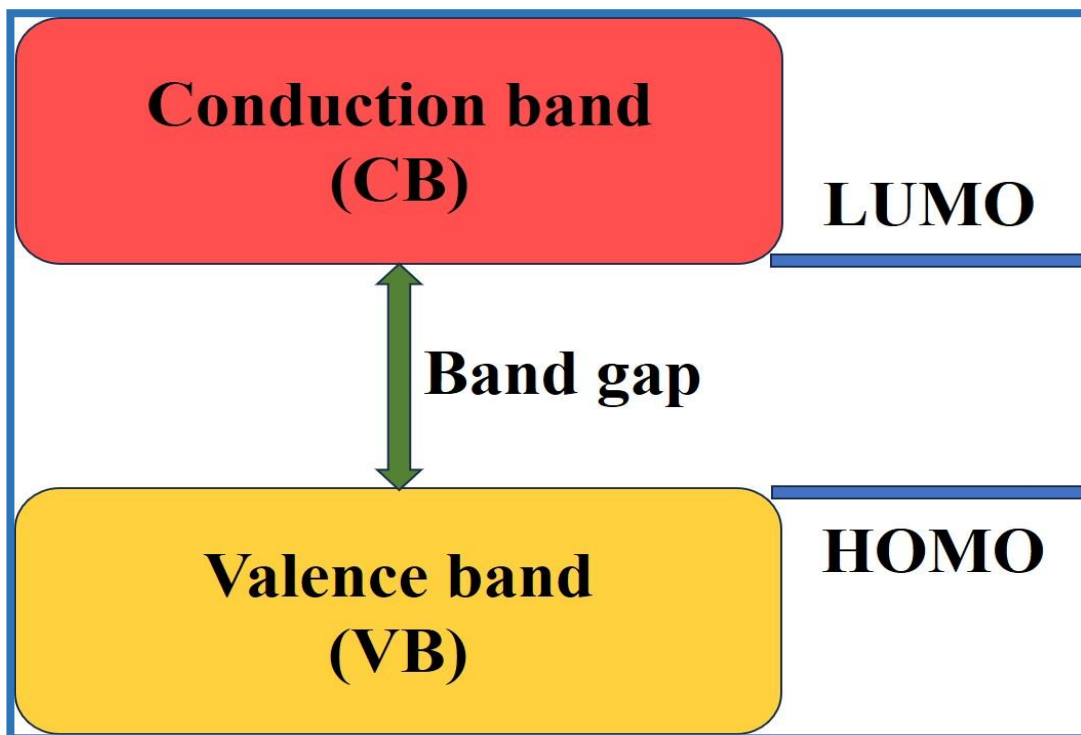


Figure 2.2 Electronically conductive polymer band structure.

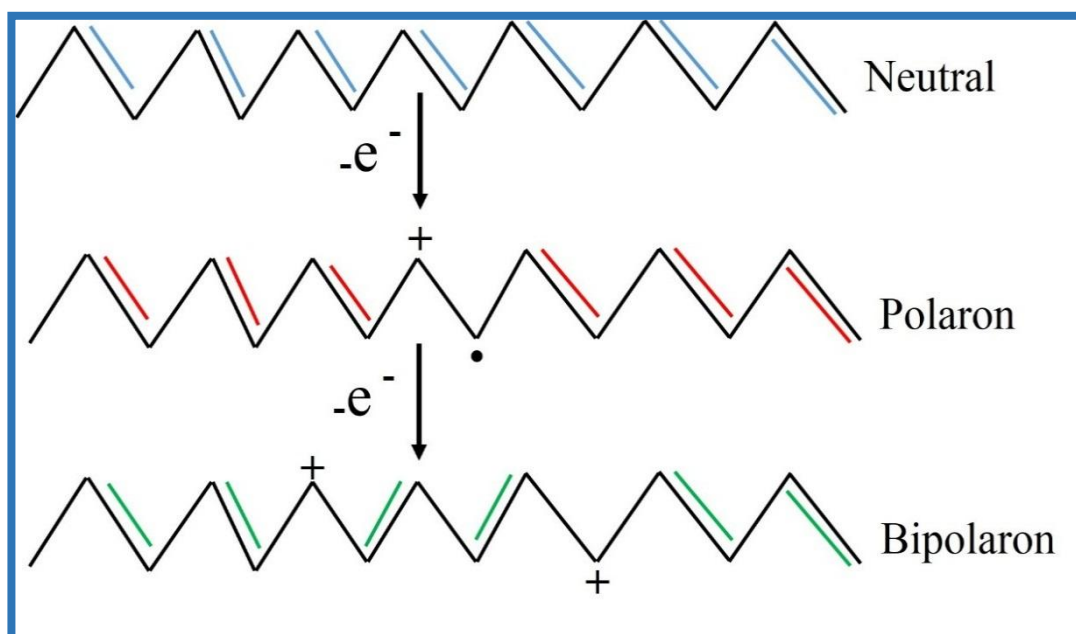


Figure 2.3 Illustrates the process of polaron and bipolaron formation in polyacetylene.

## **2.6 Linear Optical Properties of Nanocomposites**

Linear optical properties of nanocomposites refer to the interaction of light with these materials, characterized by their refractive index, absorption, and transmission spectra. These properties are significantly influenced by the size, shape, and distribution of the nanoparticles within the composite, as well as the nature of the matrix material. Nanocomposites often exhibit enhanced optical features such as increased transparency, improved light absorption, and tailored refractive indices, making them suitable for photonics, optoelectronics, and sensing applications. The precise control over these properties can lead to advancements in developing materials for lenses, coatings, and advanced optical devices.

### **2.6.1 Linear Optical Properties of Polystyrene**

Polystyrene (PS) is one of the more exciting polymers that has garnered much attention. PS garnered attention because of its unique optical properties and outstanding thermal and chemical stability. Excellent optical transparency, superior electrical insulation, strong heat resistance, low density, exceptional mechanical durability, and simplicity of manufacturing and casting were among PS many benefits. Due to these qualities, it is necessary for a wide range of commercial applications, including electronics, extruded sheets, and product packaging [41]. Despite all of these advantages, some limitations exist, such as its extreme flammability and intense flow during combustion. Some solutions were presented to overcome such problems. One method is to mix PS with one, two, or more nanoparticles with varied physical properties to improve the properties of the resulting polymeric materials. Using the nanocomposites approach, developing PS-new materials with enhanced properties is a different way to solve PS weaknesses. A few previous studies have used multiple kinds

of inorganic and organic nanoparticles as fillers to enhance the thermal stability of PS polymers [42].

### **2.6.1(a) Linear Optical Properties of Polystyrene with Single Nanoparticle**

A review of nanocomposites has been published for optical and magnetic applications, consisting of inorganic nanoparticles and polymer matrices (Li et al., 2010). The primary focus in nanocomposite materials typically involves the possibility of changes in optical or magnetic properties due to the reduction of particle sizes to microscopic dimensions. New, high-performance materials with a wide range of potential industrial applications can be created by combining inorganic nanoparticles with a polymer matrix [1].

Additionally, G. Nenna et al. (2012) observed that with varying ZnO concentrations (10 and 20 wt%) for both PS/ZnO NCs films, there was a drop in transmittance and a relative rise in reflectance in the 400 nm-800 nm wavelength range, which is in line with the variation in the refractive index in the same spectral range for the ZnO NPs. The nanoparticle-free, pure PS layer shows an extraordinarily high transmission (over 90%) across the complete measured wavelength range, which ranges from 2500 nm to 250 nm. A refractive index of approximately 1.58 was determined for the PS [43].

Besides, Suresh I. Kattimuttathu et al. 2015 produced graphene oxide-polystyrene (PS/GO NCs) as films. They used reflectance spectroscopy to further study the film's self-assembly behavior. This method reveals a red shift in reflectance as the concentration of GO loading increases [44].

Researchers Singh N.L. et al. (2018) utilized a straightforward casting method to fabricate nanocomposite films of PS and aluminum oxide ( $\text{Al}_2\text{O}_3$ ). Films that were synthesized were studied using photoluminescence (PL), ultraviolet (UV)-visible spectroscopy, and Fourier transform infrared (FTIR) spectroscopy. A new carbonyl group showed up in the FTIR spectra, confirming that the filler and polymer matrix had a charge transfer process. The band gap in the synthesized polymer nanocomposite films was found to decrease as the filler concentration increased [45].

Similarly, Monika Barala et al. (2019) developed a foil for PS/ZnO NCs. The transmittance and absorbance of these foils were measured using UV-vis spectroscopy. Transmittance spectra reveal a low transmittance in the UV band that is inversely proportional to the concentration of ZnO NPs in these composites. These nanocomposite foils were discovered to be very transparent in the visible area while absorbing UV radiation. The observation underlines the potential of these foils in UV shielding applications [46].

On the other hand, Anna Krzywicka and Elzbieta Megiel (2020) made a thin film of PS/PVA/Ag NCs. They investigated the material optical properties, especially absorption. The absorption spectra of Ag/PS/PVA NCs show two bands characteristic of polystyrene in the UV spectrum at 220 and 260 nm [47]. Table 2.1 summarizes the literature on polystyrene with a single material nanoparticle.

Table 2.1 Summary of previous review articles on polystyrene with a single material nanoparticle

Authors	Nanoparticles	Method	Studied optical properties
P. C. Haripadmam et. al. 2014 et. al. [48].	ZnO	Spin and dip coating techniques	UV–Visible absorption spectra, and PL spectra
Alwan N. Jassim et. al. 2016 [49].	ZnO	Casting method	FT-IR spectroscopy, Transmittance, and Absorption
B. Troudi et al. 2018 [50].	CuO	Spin coating technique	Absorption, band gap energy, photoluminescence
Ambesh Dixit et.al. 2021[51].	ZnO	Casting method	Examples of optical characteristics are photoluminescence, transmittance, and absorption.
H.M. Abomostafa 2021 [52].	Ni	Casting method	These parameters include optical conductivity, refractive index, band gap energy, reflectance, and the real and imaginary constants of the dielectric constants.
Maneesha Garg et. al. 2023 [53].	ZnO	Casting method	Absorption, band gap energy, and absorption coefficient
M. Iqbal et. al. 2024 [54].	Ag, Ag <sub>2</sub> O, Zn, ZnO, Fe, and Fe <sub>2</sub> O <sub>3</sub>	Casting method	FT-IR spectra, and Absorption

### 2.6.1(b) Linear Optical Properties of Polystyrene with Bimetallic Nanoparticle

The methods used to prepare and analyze polystyrene with gold and silver nanoparticles (Raid A. Ismail et al., 2017). Using the drop-casting process, the PS matrix changed with Ag and Au NPs. FT-IR and UV-Vis spectroscopy examined the optical characteristics of the polystyrene films mixed with Au and Ag NPs. Adding Ag NPs to the PS film raised the optical energy gap from 2 to 3.4 eV, while adding Au NPs increased it to 3.5 eV [55].

Furthermore, nanocomposites of PS/ZnO NCs and PS/ZnO/Fe<sub>3</sub>O<sub>4</sub> were created in 2018 by R. Suganya and N. Krishnaveni using a hydrothermal synthesis method.

Expressly, the existence of many functional groups in the end product was established by Fourier transform infrared spectra.

Polystyrene, ZnO, and ferric oxide nanocomposites are shown in the UV-visible spectra. The UV-visible spectra at 345 nm show that the absorption of PS/ZnO NCs increases as the concentrations of Fe<sub>3</sub>O<sub>4</sub> increase. They show that the energy gap for PS/ZnO is 3.5 eV and decreases with increasing iron concentration in PS/ZnO/Fe<sub>3</sub>O<sub>4</sub> NCs. Due to its extensive surface area, the PS/ZnO NCs combination energy band gap was linearly lowered with the addition of Fe<sub>3</sub>O<sub>4</sub> [56].

The unique PS/Nb<sub>5</sub>Si<sub>3</sub>/ZnS nanostructures films described by A. Hind et al. (2022) have enormous potential as optical and nanoelectronics materials. The optical and electrical properties that were studied included electron affinity, total energy, ionization potential, and HOMO/LUMO energies. Potential applications for PS/Nb<sub>5</sub>Si<sub>3</sub>/ZnS nanostructures in photonics, semiconductors, and optical nanodevices stem from their exceptional spectroscopic characteristics. Their energy gap is 1.306 eV [57].

Composite synthesis from polystyrene, zinc sulphide, and silicon bromide has distinct advantages over other structures films, according to research by Hind Ahmed and Ahmed Hashim (2023), which synthesize them excellent for use in a wide range of electrical and optical nanodevices. Research on PS/ZnS/SiBr<sub>4</sub> composites focused on their electrical and spectral properties. Electron density, electronic softness, ionization energy, total energy gap, and HOMO/LUMO energies were among the optical and electronic properties. The PS/ZnS/SiBr<sub>4</sub> composites showed good optoelectronics properties and an energy gap of around 2.12 eV, suggesting they might be used in various photonics and optics nanodevices [58].

In the same way, Using the simple casting technique, gallium-doped ZnO/polystyrene was made (S. Alamdari et al., 2023) evaluation of the produced samples using UV-Vis, PL, and FTIR. MB was utilized to study the photo-catalytic degradation performance of PS/(ZnO+AgNO<sub>3</sub>) NCs to understand how well bare nanopowders removed dye pollutants. Under room temperature UVA light, the absorptive intensity of methylene blue (MB) in the solution decreased with increasing reaction time [59]. Table 2.2 summarizes the literature on polystyrene with a bimetallic material nanoparticle.

Table 2.2 Summary of previous review articles on polystyrene with a bimetallic material nanoparticle.

Authors	Nanoparticles	Method	Studied optical properties
Iis Nurhasanah et al. 2015 [60].	Zn/CeO <sub>2</sub>	precipitation process	Absorption
Xiu Li et al.2017 [61].	ZnO/Ag	Radio-frequency (RF) magnetron sputtering method	Absorption and SEM images
J. Yang et.al. 2020 [62].	Ag/Al <sub>2</sub> O <sub>3</sub>	Magnetron sputtering system	Absorption, refractive index, and changing the thickness
Sarkawt A Hussen 2020 [63].	Sn/ZrO <sub>3</sub>	Casting methodology	Optical parameters, for instance, refractive index (n), optical band gap energy (E <sub>g</sub> ), optical dielectric loss(ε''), and optical dielectric constant(ε')
Amjed Mirza Oda et. al. 2020 [64].	ZnO-Ag	Casting methodology	Absorption, and FTIR
Tingting Yao et al. 2022 [65].	ZnO: Al <sub>2</sub> O <sub>3</sub>	liquid phase and magnetron sputtering	Transmittance, reflection, optical band gap energy, and SEM
Arshad Fadhil Kadhim and Ahmed Hashim, 2023 [66].	SiO <sub>2</sub> /SrTiO <sub>3</sub>	Casting methodology	Optical conductivity, absorption coefficient, refractive index, extinction coefficient, and dielectric constants' real and imaginary parts

## **2.6.2 Linear Optical Properties of Poly (methyl methacrylate)**

The PMMA polymer was first discovered in the early 1930s by British scientists Rowland Hill and John Crawford. A thermoplastic polymer with excellent chemical, impact, and weather resistance, PMMA can replace inorganic glass in many applications. Optical materials, sensors, vehicular fields, solar, electronics, display units, medical research, pneumatic actuation, and many more industries find uses for PMMA due to its hardness, low weight, and color diversity [67]. Polymethyl methacrylate, or PMMA, is an unusually shaped polymer made from the methyl methacrylate monomer. PMMA has a density of half that of glass at room temperature, at 1.17-1.20 g cm<sup>-3</sup>. The melting point was 220-240 °C, and the glass transition temperature was 100 °C to 120 °C for PMMA [68].

### **2.6.2(a) Linear Optical Properties of Poly (methyl methacrylate) with a Single Nanoparticle**

Anžlovar et al. (2011) reviewed synthesized methods for ZnO NPs of different forms, sizes, and surface modifications and a preparation procedure for PMMA/ZnO NCs. The original surface and the altered nano ZnO were also manufactured to create the PMMA/ZnO NCs. According to the UV-Vis absorption spectrum, the samples absorbed almost 80% of the incoming UV light [69].

On the other hand, Bahaa H. Rabee and Baira Abd Al-Kareem's (2016) optical characteristics of PMMA were examined after adding copper oxide nanoparticles. To achieve this goal, many samples were made utilizing the casting method and various weight percentages of copper oxide nanoparticles. The absorption spectra were recorded between 300 and 1000 nm in wavelength.

The results demonstrate that when the concentration of copper oxide nanoparticles increases, the following properties of PMMA/CuO NCs are enhanced: absorption coefficient, extinction coefficient, refractive index, and real and imaginary dielectric constants. Increasing the quantity of copper oxide nanoparticles causes a reduction in the energy band gap of PMMA/CuO NCs [70].

However, Sanjeev K. et al. (2020) study examined organic bistable memory devices utilizing the sol-gel spin coating process, including ZnO NPs embedded in PMMA/ZnO NCs. The band gap of ZnO-PMMA thin films was found to be 3.07 eV, which is lower than that of pure ZnO, which is 3.20 eV. According to previous research [71], the Zn-O bond in PMMA/ZnO NCs thin films was detected at  $540\text{ cm}^{-1}$ , while the ester carbonyl C=O stretch vibration of PMMA was found at  $1766\text{ cm}^{-1}$ .

In a study by Hanna B. et al. 2022 of synthetic methods for ZnO, researchers examined the optical characteristics of PMMA/ZnO NCs films using UV-visible absorption spectroscopy. According to their visible and UV absorption spectra, nanocomposite films made of PMMA and ZnO exhibited enhanced absorption in the ultraviolet spectrum between 300 and 400 nm. In visible light, the films showed no obvious grain. It is well-known that visible light emission results from flaws in the surface of ZnO. The samples were prepared using the physical mixing method [72].

Table 2.3 demonstrates that various preparation methods, the most important of which is casting, were used to mix PMMA polymer with a single metal, such as TiO<sub>2</sub>, ZnO, FeCl<sub>3</sub>, Ag, BiFeO<sub>3</sub>, and ZrO<sub>2</sub>. After the energy gap had been determined, the optical characteristics of the nanocomposite, specifically its absorption and transmission, were studied. Table 2.3 summarizes the literature on Poly (methyl methacrylate) with a single material nanoparticle.

Table 2.3 Summary of previous review articles on Poly (methyl methacrylate) with a single material nanoparticle.

Authors	Nanoparticles	Method	Studied optical properties
Xiangfu Menga et al. 2011 [73].	TiO <sub>2</sub>	Casting method	FTIR, transmission electron microscopy, and ultraviolet-visible absorption spectroscopy are used
R. B. Choudhary et al. 2016 [74].	ZnO	Polymerization technique	Absorption, and FTIR
Aliya Nur Hasanah et al. 2018 [75].	FeCl <sub>3</sub>	Synthesized via phase inversion	UV-visible spectrophotometer measured the absorption
Giorgio Giuseppe Carbone et al. 2019 [76].	Ag	Casting method	Absorption
Paramjit Singh et al. 2021 [77].	TiO <sub>2</sub>	synthesized via simple solution mixing	Absorption, and optical energy band gap
Adel M. El Sayed, 2022 [78].	BiFeO <sub>3</sub>	Casting method	These are the optical parameters: dielectric constant, extinction coefficient, transmittance, and optical band gap
N. C. Horti et al. 2024 [79].	ZrO <sub>2</sub>	Casting method	Absorption, and energy band gap

### 2.6.2(b) Linear Optical Properties of Poly (methyl methacrylate) with a Bimetallic Nanoparticle

In a 2018 study, S. Ananthakumar and colleagues used doped ZnO quantum dots in PMMA polymer to create a simple multilayer hybrid coating that may be used to develop active-interface layers for solar radiation management. This coating has multiple functionalities, including UV shielding, IR reflectance, photochromic properties, and photoluminescence. The initial method for synthesizing Sn-doped ZnO quantum dots was a straightforward sol-gel technique helped by microwaves. Coatings with many layers were developed and improved to better absorb ultraviolet light and provide near-infrared protection [80].

In their 2019 publication, Viorica Musat et al. detail the development of novel hybrid thin films that mix a PMMA matrix with Ag: ZnO NPs dispersed in chitosan, all achieved by a modified sol-gel process. The created hybrid films show great promise for transparent bioelectronics, with a suitable optical transmittance of 90% in visible and near-infrared areas and optical band gap values ranging from 3.543 to 3.737 eV [81].

Moreover, films containing SnS<sub>2</sub>, Sn<sub>0.75</sub>Fe<sub>0.25</sub>S<sub>2</sub>, and Sn<sub>0.75</sub>Cr<sub>0.25</sub>S<sub>2</sub> NPs were created by M. H. Abdel-Kader and Mohamed Bakr Mohamed in 2020 using thermolysis and casting techniques. Variations in the position and the strength of the usual absorption peak provide conclusive proof of the creation of novel nanocomposite films. Composites containing SnS<sub>2</sub>, SnS<sub>2</sub>/Cr, or SnS<sub>2</sub>/Fe have a more incredible activation energy than PMMA polymers without SnS<sub>2</sub>. The importance of the intermediate semiconductor material was highlighted by the fact that PMMA doped with SnS<sub>2</sub>/Fe displayed the highest absorption values compared to the other doped samples. Based on the study's findings, the samples show promise as solar cell applications and UV shielding materials for UVB and UVC types of ultraviolet light but not for UVA, located in the 315-400 nm region of the UV spectrum [82].

However, polymer nanocomposite films were created in 2021 by Priyanka Dhatarwal and colleagues using PMMA as a matrix and nanoparticles of Al<sub>2</sub>O<sub>3</sub> and SiO<sub>2</sub> scattered throughout at 1, 3, and 5 wt%. The solutions were sonicated and then magnetically stirred to produce uniform nanoparticle suspensions in size and shape. The next step was to pour one PMMA nanofiller solution and various viscous-type hybrid polymeric solutions into Petri dishes. The dishes were then left to dry at RT. There was a small change in the UV-Vis absorption, transmittance, and reflectance spectra as the percentages of Al<sub>2</sub>O<sub>3</sub> and SiO<sub>2</sub> in these films of polymer nanocomposite

materials rose. The energy band gap, refractive indices, and optical conductivity of composites are all improved when the filler concentration is high [83].

Table 2.4 displays the various preparation methods, including casting, that were used to mix bimetallic material nanoparticles with PMMA polymer. These nanoparticles included Au-Pt, ZnO/Silicone acrylate, CdSe-CdS/Ag, Mn: ZnS, ZnO/SnO<sub>2</sub>, and CNPs/CuCo<sub>2</sub>O<sub>4</sub>. Absorption, transmittance, and FTIR were among the optical properties investigated for the nanocomposite. Table 2.4 summarizes the literature on Poly (methyl methacrylate) with a bimetallic material nanoparticle.

Table 2.4 Summary of previous review articles on Poly (methyl methacrylate) with a bimetallic material nanoparticle

Authors	Nanoparticles	Method	Studied optical properties
Eda Ozkaraoglu et al. 2009 [84].	Au and Au–Pt alloy	Casting method	Absorption
Wenjuan Liao et al. 2012 [85].	ZnO/Silicone-acrylate	Casting method	Transmittance and FTIR
Ming-Chung Wu et al. 2020 [86].	CdSe-CdS/Ag	Electrospinning technique	Absorption, photoluminescence
Mallikarjun H. Anandalli et al. 2023 [87].	Mn: ZnS	Casting technique	Absorption, energy band gap, refractive index, absorption coefficient, and extinction coefficients
Rozaitunmas Jamal et al. 2023[88].	Au-Ag	Deposition	Absorption
Nevena Čelić et al. 2023 [89].	ZnO/SnO <sub>2</sub>	Casting technique	Transmittance
A. M. El-Naggar et al. 2024 [90].	CNPs/CuCo <sub>2</sub> O <sub>4</sub>	Casting technique	Refractive index, optical conductivity, band gap energy, absorption, and optical dielectric constant

### 2.6.3 Linear Optical Properties of Poly (vinyl alcohol)

The synthetic polymer known as polyvinyl alcohol, or PVOH has excellent film-forming capabilities, is biodegradable, and is a solvent in water. The process